First principles modelling of the elastic properties of $CoCrFe_xMn_{(40-x)}Ni$ alloys

K. A. Osintsev, *PhD in Engineering, Postdoctoral Researcher*[1], *e-mail: kirosintsev@gmail.com*
V. S. Panova, *Junior Researcher*[2], *e-mail: panova_vs@sibsiu.ru*
S. V. Konovalov*, *Professor, Doctor of Technical Sciences, Vice-Rector for Research and Innovation*[2], *e-mail: konovalov@sibsiu.ru*
I. A. Panchenko, *Candidate of Technical Sciences, Head of the Laboratory of Electron Microscopy and Image Processing*[2], *e-mail: i.r.i.ss@yandex.ru*

[1] *Institute of Laser and Optoelectronics Intelligent Manufacturing, Wenzhou University, Wenzhou, China.*
[2] *Siberian State Industrial University, Novokuznetsk, Russia.*

In this paper the elastic properties of $CoCrFe_xMn_{(40-x)}Ni$ alloys (x = 5, 10, 15, 20, 25, 30, 35 at.%) were studied using the virtual crystal approximation (VCA) method in the Quantum Espresso software at 0 K temperature. The aim of the study was to determine the applicability of this method to high entropy alloys of the Co – Cr – Fe – Mn – Ni system and to investigate the influence of Fe and Mn content on lattice parameters and elastic properties. The results showed that the lattice parameters calculated by the VCA method were on average 4% lower than those of the cast samples obtained by XRD analysis. The method showed a tendency for the lattice parameter to decrease with increasing Fe content and decreasing Mn from 3.458 Å to 3.450 Å (0.3% decrease), which is in agreement with the experimental data. However, the calculated values of Young's modulus exceed the experimental values by an average factor of two, indicating that the accuracy of the method for estimating the absolute values of elastic moduli is insufficient. The Young's modulus calculated by the VCA method decreases from 457 GPa to 431 GPa as the Mn content increases and the Fe content decreases. However, experimental findings reveal a more intricate behaviour of the elastic modulus variation, with maximum values attained in alloys containing 35 and 5 at.% Fe, and minimum values observed in alloys approaching equiatomic concentration. Consequently, the VCA method enables the estimation of the direction of change in lattice parameters and elastic properties; however, it is limited in determining their absolute values.

Key words: density functional theory, virtual crystal approximation, elastic properties, high-entropy alloy, elastic constants.

DOI: 10.17580/nfm.2025.01.10

Introduction

High-entropy alloys (HEAs) consisting of five or more elements with varying concentrations ranging from 5 to 35 at.% exhibit unique physical and mechanical properties, including high strength, corrosion resistance, wear resistance and thermal stability [1, 2]. The most extensively studied HEA is the equiatomic alloy CoCrFeNiMn, also referred to as the Cantor alloy [3]. Notwithstanding its intricate chemical composition, this alloy is a single-phase solid solution with a face-centered cubic lattice (FCC) structure, which endows it with exceptional ductility (elongation up to ~60% at T = 293 K and ~85% at T = 77 K) and fracture toughness over a broad temperature range [4]. However, the yield strength and tensile strength of Cantor alloy are relatively low: at room temperature, the tensile strength is 660 MPa, which limits its potential applications [4, 5]. Therefore, it is essential to increase the strength of alloys of this system without increasing brittleness.

The broad spectrum of element combinations present in HEAs poses significant challenges to property optimisation, necessitating the employment of theoretical modelling techniques. Density functional theory (DFT) facilitates the prediction of material properties from "first principles", a technique that has emerged as a potent instrument in the realm of modern materials science [6]. One of the methods that allows us to find the best approximation of the model to the disordered structure is the method of special quasi-random structures (SQS) [7]. However, a significant disadvantage of this method is the need for costly computations, which limits its use for high-performance search of new compositions among a large number of variants.

A less costly method is the coherent potential approximation (CPA), which facilitates the modelling of disordered structures by introducing an effective medium to simulate the changing potential of different atoms in the alloy. This approach enables the calculation of interactions between pairs of atoms in real or inverse space. However, the main disadvantage of this approximation

*Correspondence author.

is that it cannot take into account lattice distortions that may affect the elastic properties [8].

In order to enhance the CPA method, the EMTO-CPA (exact muffin-tin orbital) approach has been put forward. This approach incorporates the inter-domain contribution to the potential and has been demonstrated to be efficacious in the calculation of the physical parameters of alloys [9]. To illustrate, the efficacy of the method has been demonstrated in the calculation of physical parameters. These include, but are not limited to, lattice constants, elastic constants, elastic moduli and other mechanical properties in FeCoCrNiMnx alloys as a function of Mn content ($0 \le x \le 3$) [10].

In this paper, the virtual crystal approximation (VCA) method is utilised, which has been demonstrated to reduce calculation time by averaging the multicomponent system as a virtual atom defined by a linear combination of elements in terms of concentration [11]. It has been demonstrated that VCA is less demanding in terms of resources than supercell methods (SQS), and that it is easier to implement than CPA and EMTO-CPA. Furthermore, it allows for rapid assessment of the effects of components on material properties. Nevertheless, the model exhibits inferior accuracy in predicting the properties of materials. Its application is therefore limited to small differences in the radii of atoms of components (no more than 3%), since averaging will otherwise lead to significant deviations in the properties [12].

The objective of this study is to ascertain the applicability of the virtual crystal approximation method for high-entropy alloys of the Co – Cr – Fe – Mn – Ni system and to elucidate the regularities of elastic properties changes depending on the Fe and Mn content.

Materials and methods

In order to facilitate a comparison between the results obtained by the VCA method and to evaluate its applicability for calculating the elastic properties of alloys, six samples of cast alloys of the following non-equiatomic composition were fabricated: $CoCrFe_xMn_{(40-x)}Ni$ ($x = 5$, 10, 15, 25, 30, 35 at.%). The fabrication of the equiatomic alloy was not a primary objective of this study; however, its properties were compared on the basis of the results of previous experimental studies. Pure metals in the form of powders (99.99 at.%) were utilised as the fundamental materials in the production of cast specimens of Co, Cr, Fe, Mn and Ni. The melting of the alloy samples was conducted in the induction furnace VIP-010, utilising a corundum crucible with a capacity of 10 kg.

In order to ascertain the lattice parameter, as well as to determine the phase composition of the fabricated alloys, *X*-ray phase analysis was applied using a Shimadzu XRD 6000 diffractometer according to the symmetrical Bragg-Brentano scheme. Imaging was performed in filtered Fe – $K\alpha_1$ radiation in the range of 2θ angles from 40° to 140° at tube voltage and current values of 30 kV and 30 mA, respectively. The scanning step was 0.02°, with a scanning speed of 2°/min and a dwell time of 0.6 c.

The modulus of elasticity was determined by nanoindentation at room temperature on a NanoScan-4D instrument in accordance with GOST R 8.748–2011 (ISO 14577-1:2015). The indenter used was a diamond trihedral Berkovich pyramid with an angle at the apex of 140° and a tip radius of ~50 nm. The peak load was set at 100 mN, and the duration of loading, unloading, and maintaining the maximum load was 10 seconds. The cast specimens were cut using an electrical discharge machine and then polished with cloth and diamond slurry, which had an abrasive particle size of 2.5 μm. The etching process was carried out in a reagent consisting of HNO_3 and HCl in a 1 : 3 ratio at room temperature. Indentation was performed on a 5×5 grid, with an area of 500×500 μm. The elastic modulus values were averaged over 25 measurements, and confidence intervals were calculated at a 95% confidence level.

The elastic properties of $CoCrFe_xMn_{(40-x)}Ni$ alloys (x = 5, 10, 15, 20, 25, 30, 35 at.%) were calculated using density functional theory methods in the Quantum Espresso v.7.3 software package [13]. The modelled structures were calculated with consideration for their paramagnetic state, as established in prior studies of the CoCrFeMnNi alloy [10, 14]. The Optimized Norm-Conserving Vanderbilt (ONCV) SG15 pseudopotentials were used [15]. The mixing of pseudopotentials to create a "virtual crystal" was performed in the virtual_v2.x program [13]. The structure with face-centered cubic (FCC) lattice was used as the initial crystallographic information.

In order to guarantee the precision of the calculations of the elastic properties and lattice parameters of the modelled alloys, the convergence of the results was examined. **Fig. 1, *a*** demonstrates the relationship between the total energy of the crystal structure and the kinetic energy of the wave function cutoff, and **Fig. 1, *b*** illustrates the relationship between the total energy of the crystal structure and the number of points for space discretisation (k-points). Based on the results of the convergence tests, a kinetic energy of 150 Ry was selected for the purpose of cutting the wavefunctions, thereby ensuring a total energy calculation accuracy of 10^{-7} Ry. To discretise the space, a Monkhorst-Pack grid with a size of 35×35×35 = 42875 k-points was deemed to be the most appropriate approach. The accuracy of the total energy self-consistency procedure was set to 10^{-10} Ry, and the forces acting on the atoms did not exceed 10^{-6} Ry/a_0. The total time required to perform the calculations for the seven modelled alloys was 104 hours, including 12 hours of convergence tests. The calculations were executed by utilising the computing resources of the Centre of Digital Competences of Siberian State Industrial University. The calculations were performed on an electronic computer equipped with an Intel(R) Core(TM) i7-9700F CPU 3.00 GHz processor and 100 GB of random-access memory. The calculations were executed using a parallelisation approach across eight cores.

The bulk modulus of the modelled alloys was calculated in the Gibbs2 and ElaStic software at a temperature of

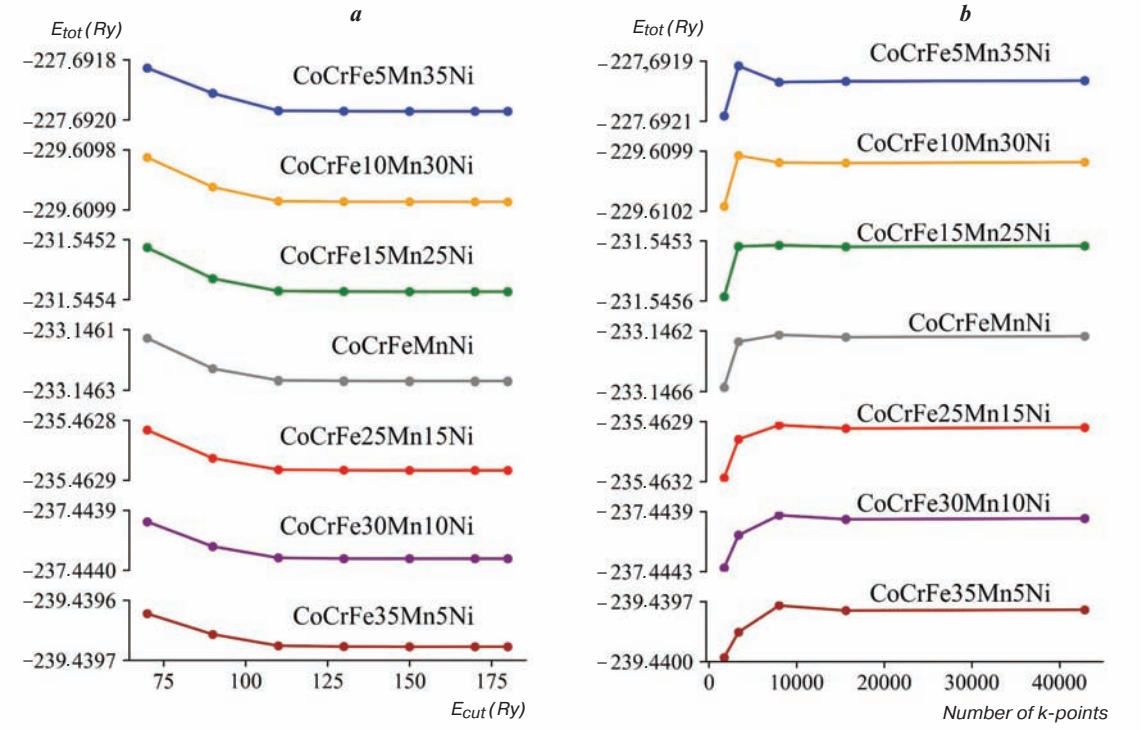

Fig. 1. Dependence of the values of the total energy, E_{tot}, of the modelled $CoCrFe_xMn_{(40-x)}Ni$ alloys ($x = 5, 10, 15, 20, 25, 30, 35$ at.%) on (*a*) the kinetic cutting energy of the E_{cut} wave function and (*b*) the number of *k*-points

0 K [16–18]. In the first case, the equation of state (EOS) in the Burch-Murnaghan parameterisation was used to study the effect of pressure on the alloy structure [19]. The parameters of the equation were determined by fitting the following analytical expression to the calculated curve of energy dependence on the unit cell volume *E(V)* [20]:

$$E(V) = E_0 + \frac{9V_0B_0}{16}((x^{-2}-1)^3B_1 + (x^{-2}-1)^2 \times \times(6-4x^{-2})), \quad (1)$$

where $x = (V/V_0)^{1/3}$, $B_0 = -V(\partial P/\partial V)_T$ is the isothermal bulk modulus, $B_1 = (\partial B/\partial P)T$ is its first pressure derivative at $x = 1$. The values E_0, V_0, B_0 and B_1 represent the four parameters of the equation of state (1), and they are defined as follows: V_0 is the volume at the energy minimum, E_0 is the depth of the curve $E(V)$, B_0 and B_1 determine the shape of the curve. The value of the bulk modulus B_0, as determined by this EOS, will henceforth be denoted as B_{EOS}.

In the second case, the bulk modulus, along with the elastic constants and other elastic moduli, were calculated in the framework of the Lagrange theory of elasticity [16]. In this theory, the solid is considered to be a homogeneous elastic medium, in which strain and stress are represented as symmetric second-rank tensors. The Lagrange strain, denoted here by η, and the Lagrange stress, denoted here by τ, are defined as

$$\eta = \epsilon + \frac{1}{2}\epsilon^2, \quad (2)$$

$$\tau = det(1+\epsilon)(1+\epsilon)^{-1} \cdot \sigma \cdot (1+\epsilon)^{-1}, \quad (3)$$

The symbol "(·)" is used to denote the tensor product. The physical strain tensor, denoted "∈", is defined as the transformation of the position vector "*r*" into "(1 + ∈) – *r*" in Cartesian coordinates. The physical stress tensor, denoted "σ", is defined through differentiation of the total energy, "*E*":

$$\sigma = \frac{1}{V}\frac{\partial^2 E}{\partial \epsilon^2} \quad (4)$$

The *V* is the volume of the crystal. In the linear regime, there is a well-established relationship between the stress and strain of a material, as measured by the generalised Hooke's law:

$$\tau = \Sigma^3_{k,\,l=1} c_{ijkl}\eta_{kl} \quad (5)$$

The coefficients c_{ijkl} are defined as the elastic constants of the crystal and represent the components of the fourth-rank stiffness tensor *c*.

As demonstrated in equation (5), the elastic constants can be expressed as follows:

$$c_{ijkl} = \frac{\partial_{\tau\alpha}}{\partial_{\eta\beta}}\bigg|_{\eta=0} \quad (6)$$

The calculation of second-rank elastic constants through first-principles methods is based on a technique originally developed by Nielsen and Martin [21]. This

approach is favoured for utilisation in software capable of calculating the stress tensor. Notably, it is incorporated within the Quantum Espresso software suite, which has been employed in the present study.

The Hill averaging method was employed in accordance with the Voigt and Reuss methods, which facilitate the estimation of the range of possible values of the elastic moduli of polycrystalline materials [22]. The Voigt approximation provides asymptotically maximum values of the bulk moduli B_V, B_R and shear moduli G_V, G_R, while the Reuss method provides minimum estimates of these parameters [23, 24]:

$$B_V = B_R = (C_{11} + 2C_{12})/3\,, \tag{7}$$

$$G_V = (C_{11} - C_{12} + 3C_{44})/5\,, \tag{8}$$

$$G_R = \frac{5(C_{11} - C_{12})C_{44}}{4C_{44} + 3(C_{11} - C_{12})} \tag{9}$$

Hill proposed the utilisation of average moduli values of polycrystalline materials, as deduced from strain energy density analysis. This approach has been demonstrated to offer a more precise depiction of the mechanical properties that fall between the two extreme estimates [25]:

$$B = \frac{1}{2}(B_V + B_R),\ G = \frac{1}{2}(G_V + G_R) \tag{10}$$

It is evident that, in consideration of these values, the Young's modulus, E, and the Poisson's ratio, μ, are defined as follows:

$$E = \frac{9BG}{3B + G},\ \mu = \frac{3B - 2G}{2(3B + G)} \tag{11}$$

The Zener anisotropy parameter was calculated by the following formula [26]:

$$A = 2\,\frac{C_{44}}{(C_{11} - C_{12})} \tag{12}$$

The experimental values of the elastic constants were determined on the basis of the values of Young's modulus, as measured by means of the nanoindentation method, and of Poisson's ratio, which was taken to be 0.26 [27]. The experimental elastic constants were calculated using the following formula:

$$C_{11} = E\,\frac{(1 - \mu)}{(1 + \mu)(1 - 2\mu)}\,, \tag{13}$$

$$C_{12} = \frac{E\mu}{(1 + \mu)(1 - 2\mu)}, \tag{14}$$

$$C_{44} = \frac{E}{2(1 + \mu)}. \tag{15}$$

Results and discussion

As illustrated in **Fig. 2, *a*** the diffractograms of the cast alloy samples under investigation are displayed. XRD analysis revealed that all alloys are single-phase solid solutions based on the FCC lattice. This finding is corroborated by the results of the diffractograms, which show intensity peaks with Miller plane indices (111), (200), (220) and (311), corresponding to the FCC lattice.

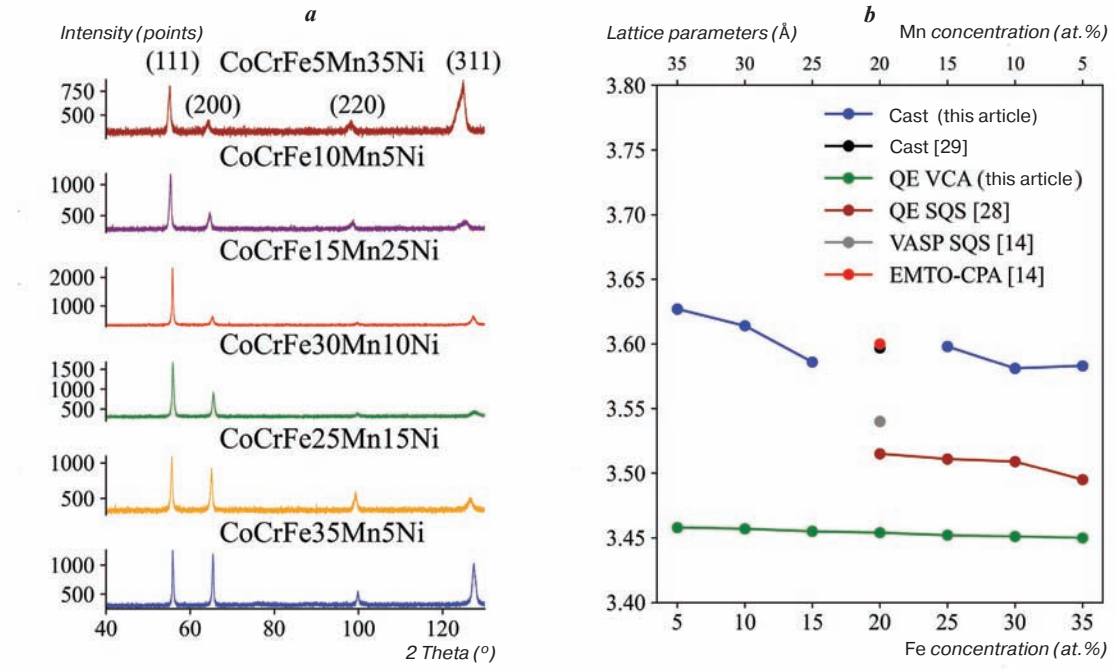

Fig. 2. Diffractograms and lattice parameters of the $CoCrFe_xMn_{(40-x)}Ni$ alloys (x = 5, 10, 15, 25, 30, 35 at.%) calculated using VCA, VASP SQS [14], QE SQS [28], EMTO-CPA [14] and experimental values obtained in this study and for the equiatomic composition of CoCrFeMnNi from [29]

As illustrated in **Fig. 2, *b***, the values of the lattice parameters were calculated using both VCA and SQS methods, implemented in the VASP and Quantum ESPRESSO (QE) programs. The experimental data is dependent on the chemical composition of the alloys. When evaluated according to the VCA method, the values of the lattice parameters exhibit minimal dependence on the Fe and Mn content. The deviation from the mean value of 3.454 does not exceed 0.13%. Concurrent increases in Fe content and decreases in Mn content result in a 0.3% reduction in the lattice parameter, from 3.458 Å to 3.450 Å This dependence is in accordance with the experimental findings, which also demonstrate a decline in the lattice parameter value by 1.2% from 3.627 Åto 3.583 Å The values calculated by the VCA method exhibit an average decrease of 4% below the experimental values of the lattice parameters. The lattice parameters obtained by the SQS method in the QE [28] and VASP [14] programs have been shown to be more closely aligned with the experimental values than those calculated by the VCA method. The discrepancy between the two sets of values is found to be 2.3% and 1.6%, respectively.

The observed decrease in the lattice parameter in experimental alloys with decreasing Mn content and simultaneous increase in Fe content may be attributable to the fact that the atomic radius of Mn (135 pm) is larger than the atomic radius of Fe (124.12 pm). Consequently, the distortion of the crystal lattice decreases. The VCA method proved incapable of reflecting the changes to the structure distortion. This is because it replaces the real atoms in the sublattice with a "virtual atom" that possesses an averaged mass [30]. Another potential reason is that the calculations were performed at 0 K, which implies the absence of phonon-phonon interactions occurring at the non-zero temperature.

As illustrated in **Fig. 3, *a***, the longitudinal C_{11}, shear C_{44} and transverse C_{12} elastic constants were calculated using the VCA method and obtained through experimental means for the alloys of the Co – Cr – Fe – Mn – Ni system. The values of C_{ij} obtained by the VCA method allow for analysis of the modelled crystals in terms of compliance with the mechanical stability conditions [31]. The mechanical stability conditions for cubic crystals are as follows: $C_{11} > |C_{12}|$, $C_{11} > 0$, $C_{44} > 0$, and $(C_{11} + 2C_{12}) > 0$ [32]. In the present work, it is demonstrated that all alloys fulfill this criteria.

The elastic constants of $CoCrFe_xMn_{(40-x)}Ni$ alloys (x = 5, 10, 15, 20, 25, 30, 35 at.%) were calculated using the VCA method, these constants exceed the experimentally determined values by a factor of 1.1–7.3. The experimental values were most closely reflected by the CoCrFe5Mn35Ni, CoCrFe30Mn10Ni and CoCrFe35Mn5Ni alloys, for which the elastic constants differed by no more than 1.3 times for C_{11}, 1.5 times for C_{12} and 2.6 times for C_{44}. The greatest discrepancy from experimental values was observed in the calculated data of CoCrFe10Mn30Ni and CoCrFe15Mn25Ni alloys, for which C_{11} was found to be 3.3–3.5 times larger, C_{12} was 3.7–3.9 times larger, and C_{44} was 6.8–7.3 times larger.

The elastic constants calculated by the VCA method remained practically unchanged with increasing Fe content from 5 to 35 at.% and the corresponding decrease of Mn concentration in $CoCrFe_xMn_{(40-x)}Ni$ alloys. An examination of the data reveals a slight increase in C_{11} by 2.5%, an increase in C_{44} by 5.4%, and a decrease in C_{12} by 4.8%. The experimental data demonstrate a more complex dependence of the elastic constants on chemical composition, which was not detected by the VCA method.

The distinction between C_{11} and C_{44} is pivotal in determining the Cauchy pressure, which is indicative of the bonding mechanism between atoms in the alloy. A negative Cauchy pressure value signifies that the material exhibits a non-metallic nature with directional bonding. The predominance of metallic bonding in the material is indicated by a positive value [33]. As demonstrated in **Fig. 3, *b***, all alloys exhibit positive values of Cauchy pressure, indicative of the strongly pronounced metallic bonding between "virtual atoms". The VCA calculation indicates an increase in the $C_{11}-C_{44}$ value with rising Fe content, concomitant with a decrease in Mn content. This can be interpreted as an enhancement in the stability of the metallic bond, which consequently leads to an improvement in ductility.

The Young's modulus calculated by VCA method increases linearly from 431.8 GPa to 457.3 GPa (by 6%) with increasing Fe content and decreasing Mn content (see **Fig. 3, *c***). However, it is important to note that the values obtained by nanoindentation do not demonstrate a linear relationship. The highest values are observed in alloys with Fe content (x = 5, 20, 30, and 35 at.%), while in alloys with Fe content (x = 10, 15, and 25 at.%) the values are lower by a factor of 3 on average. It is interesting to note that the elastic moduli of non-equiatomic alloys exceed the value for the equiatomic composition (201.6 GPa [29]), and the lowest values are observed in the alloys closest on the graph to the equiatomic one. The alloy containing 5 at.% Fe and 35 at.% Mn exhibits a 17% decrease in E value compared to the alloy with 5 at.% Mn and 35 at.% Fe. This suggests that increasing the concentrations of Fe and Mn (35 at.%) leads to an enhancement in the modulus of elasticity of alloys within the Co – Cr – Fe – Mn – Ni system.

The values of the bulk modulus, B, calculated by the VCA method using substitution into the Burch-Murnaghan equation of state (B_{EOS}) correspond to the values obtained when calculating B within the framework of the Lagrange theory of elasticity. The discrepancy between the two methods is no greater than 1%, thus validating the comparability of the results obtained by these techniques. A decline in Fe content from 35 to 20 at.% is accompanied by an increase in Mn from 5 to 20 at.%, resulting in a modest rise in B_{EOS} compressive bulk modulus

from 289.1 GPa to 289.9 GPa (0.2%). Further increases in Mn content with decreasing Fe fraction in the alloys do not significantly affect the change in bulk modulus (0.03 %).

It has been demonstrated that, for all alloys presented, the bulk modulus (*B*) exceeds the shear modulus (*G*). The *B/G* ratio has been shown to be a valuable metric for evaluating the ductility and machinability of the material in question. A *B/G* value above 1.75 has been identified as an indication of good machinability [34]. The *B/G* values calculated with VCA increase with decreasing Fe content and increasing Mn content, reaching a maximum (*B/G* = = 1.68) in the CoCrFe5Mn35Ni alloy, indicating the highest ductility of this alloy (see **Fig. 3, *d***). This prediction is comparable with the trend revealed by calculations of Cauchy pressure values.

It has been demonstrated that, upon increasing the Fe content from 5 to 35 at.% and simultaneously decreasing the Mn content in CoCrFe*x*Mn(40 – *x*)Ni alloys, the value of Poisson's ratio decreases from 0.24 to 0.22 (**Table**). This change signifies that the alloys are less prone to transverse tensile strain. The decline in μ may suggest an augmentation in the alloy's stiffness. Consequently, the modelled $CoCrFe_xMn_{(40-x)}Ni$ alloys exhibit enhanced resistance to deformation with increasing Fe content and decreasing Mn content.

Zener anisotropy (*A*) is a pivotal parameter in the characterisation of the disparities in mechanical properties

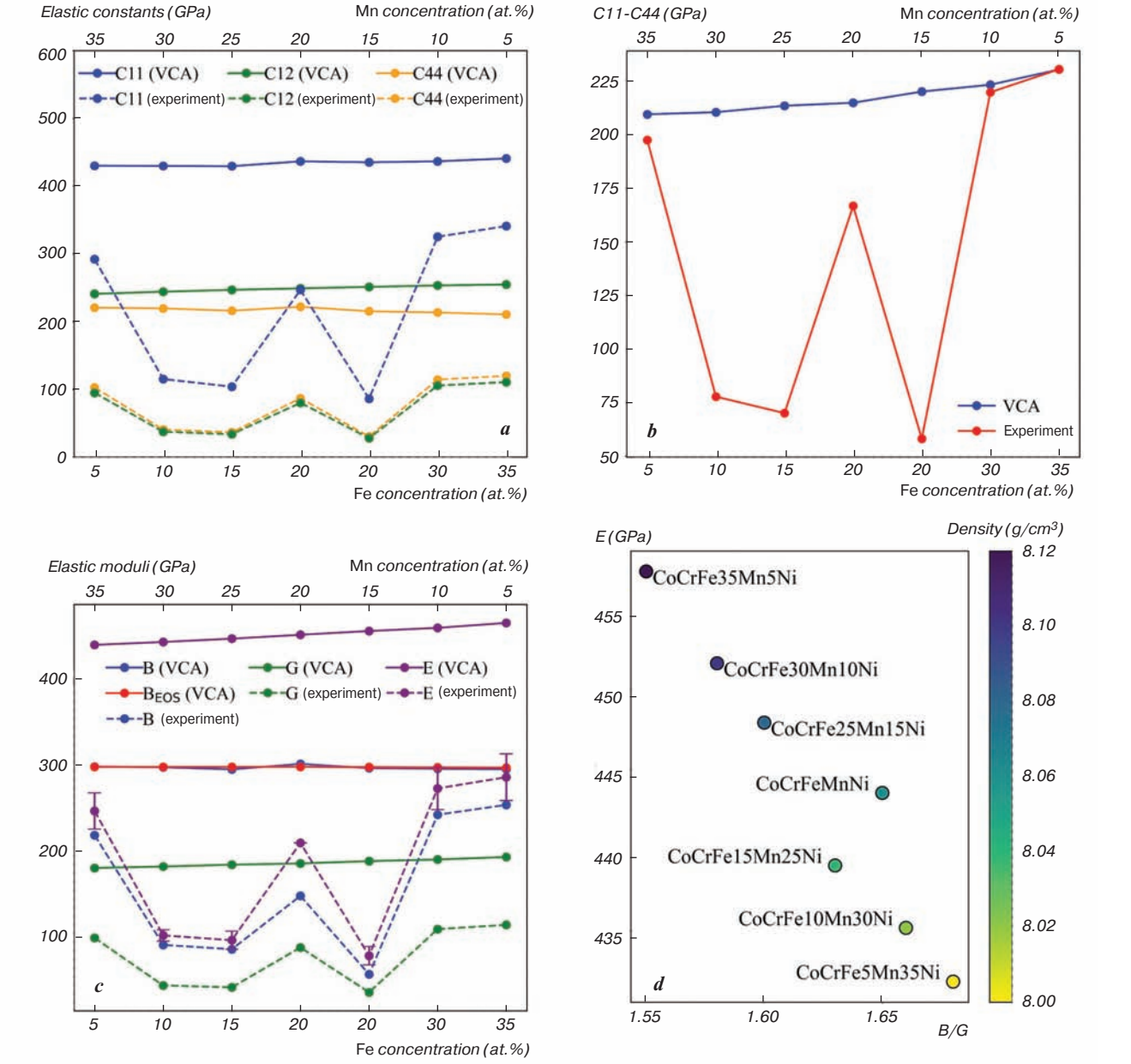

Fig. 3. Dependences of (*a*) elastic constants, (*b*) Cauchy ratios, (*c*) Young's moduli, *E*, bulk compression, *B*, and shear, *G*, (*d*) Young's moduli, *E*, *B/G* ratio, and theoretical density on Fe and Mn content in $CoCrFe_xMn_{(40-x)}Ni$ alloys (x = 5, 10, 15, 20, 25, 30, 35 at.%). The results for the equiatomic composition CoCrFeMnNi are taken from [29]

Table

Zener anisotropy parameters *A* and Poisson's ratio μ for $CoCrFe_xMn_{(40-x)}Ni$ alloys (x = 5, 10, 15, 20, 25, 35 at.%) calculated using VCA, CPA, EMTO-CPA and SQS methods

Alloy	*A*	μ
CoCrFe5Mn35Ni (VCA)	2.3	0.24
CoCrFe10Mn30Ni (VCA)	2.32	0.23
CoCrFe15Mn25Ni (VCA)	2.31	0.23
CoCrFeMnNi (VCA)	2.32	0.23
CoCrFeMnNi (CPA) [35]	3.98	0.25
CoCrFeMnNi (EMTO-CPA) [14]	–	0.313
CoCrFeMnNi (SQS)	–	0.261
CoCrFe25Mn15Ni (VCA)	2.29	0.22
CoCrFe30Mn10Ni (VCA)	2.27	0.22
CoCrFe35Mn5Ni (VCA)	2.21	0.22

of a material in various directions. The values of Zener anisotropy in alloys range from 2.21 to 2.32, thereby signifying the existence of anisotropic properties in these alloys.

Conclusion

This paper presents a first-principles study of the elastic properties of high-entropy $CoCrFe_xMn_{(40-x)}Ni$ alloys, employing the virtual crystal approximation (VCA) method.

It has been established that an augmentation in Fe content, concomitant with a diminution in Mn, results in a reduction in the lattice parameter. This finding is in accordance with the observations derived from experimentation. It has been determined that the calculated values of Young's modulus exhibit a marked increase in comparison to the experimental values. This outcome signifies the constraints imposed by the VCA method in accurately estimating the absolute values of elastic properties.

It is evident that the virtual crystal approximation method is a valuable instrument for the preliminary examination of the mechanical properties of high-entropy alloys. Nevertheless, its application for precise estimations is not feasible. Consequently, there is a necessity for additional research to be conducted on the development of methodologies that facilitate high-performance calculations and possess adequate accuracy for predicting the elastic properties of high-entropy alloys.

Acknowledgement

The present study was supported by a grant from the Russian Science Foundation (RSF), grant No. 23-49-00015 (https://rscf.ru/project/23-49-00015/). The authors would like to express their gratitude to Valentina Kuznetsova for her analysis of pseudopotentials and to Vladislav Drobyshev for his assistance with sample preparation and measurement of the elastic modulus of alloys.

References

1. Miracle D. B., Senkov O. N. A Critical Review of High Entropy Alloys and Related Concepts. *Acta Materialia*. 2017. Vol. 122. pp. 448–511.

2. Ouyang G., Singh P., Su R., Johnson D. D., Kramer M. J., Perepezko J. H., Senkov O. N., Miracle D., Cui J. Design of Refractory Multi-Principal-Element Alloys for High-Temperature Applications. *npj Computational Materials*. 2023. Vol. 9. 141.

3. Cantor B., Chang I. T. H., Knight P., Vincent A. J. B. Microstructural Development in Equiatomic Multicomponent Alloys. *Materials Science and Engineering: A*. 2004. Vol. 375-377. pp. 213–218.

4. Otto F., Dlouhý A., Somsen Ch., Bei H., Eggeler G., George E. P. The Influences of Temperature and Microstructure on the Tensile Properties of a CoCrFeMnNi High-Entropy Alloy. *Acta Materialia*. 2013. Vol. 61, Iss. 15. pp. 5743–5755.

5. Huang C.-W., Su P.-Y., Yu C.-H., Wang C.-L., Lo Y.-C., Jang J. S.-C., Hu H.-T. A Micromechanical Study on the Effects of Precipitation on the Mechanical Properties of CoCrFeMnNi High Entropy Alloys with Various Annealing Temperatures. *Scientific Reports*. 2023. Vol. 13. 3379.

6. Giustino F. Materials Modelling Using Density Functional Theory: Properties and Predictions. Oxford: Oxford University Press, 2014. 286 p.

7. Zunger A., Wei S.-H., Ferreira L. G., Bernard J. E. Special Quasirandom Structures. *Physical Review Letters*. 1990. Vol. 65, Iss 3. pp. 353–356.

8. Ferrari A., Körmann F., Asta M., Neugebauer J. Simulating Short-Range Order in Compositionally Complex Materials. *Nature Computational Science*. 2023. Vol. 3. pp. 221–229.

9. Abrikosov I. A., Nikonov A. Yu., Ponomareva A. V., Dmitriev A. I., Barannikova S. A. The Application of Method of Exact MT-Orbitals for Modelling of Thermodynamic and Mechanical Properties in Pure Components of Ti- and Zr-Based Alloys. *Uspehi Fiziki Metallov*. 2013. Vol. 14, Iss. 4. pp. 319–352.

10. Xiao H., Liu Y., Wang K., Wang Z., Hu T., Fan T., Ma L., Tang P. Effects of Mn Content on Mechanical Properties of $FeCoCrNiMn_x$ ($0 \le x \le 0.3$) High-Entropy Alloys: a First-Principles Study. *Acta Metallurgica Sinica (English Letters)*. 2021. Vol. 34, Iss. 4. pp. 455–464.

11. Orhan O. K., Isiet M., Caparini L., Ponga M. Exploring the Compositional Space of High-Entropy Alloys for Cost-Effective High-Temperature Applications. *Frontiers in Materials*. 2022. Vol. 8. 816610.

12. Wang S., Xiong J., Li D., Zeng Q., Xiong M., Chai X. Comparison of Two Calculation Models for High Entropy Alloys: Virtual Crystal Approximation and Special Quasi-Random Structure. *Materials Letters*. 2021. Vol. 282. 128754.

13. Giannozzi P., Baroni S., Bonini N., Calandra M. et al. QUANTUM ESPRESSO: a Modular and Open-Source Software Project for Quantum Simulations of Materials. *Journal of Physics: Condensed Matter*. 2009. Vol. 21, Iss. 39. 395502.

14. Zaddach A. J., Niu C., Koch C. C., Irving D. L. Mechanical Properties and Stacking Fault Energies of NiFeCrCoMn High-Entropy Alloy. *JOM*. 2013. Vol. 65, Iss. 12. pp. 1780–1789.

15. Hamann D. R. Optimized Norm-Conserving Vanderbilt Pseudopotentials. *Physical Review B*. 2013. Vol. 88, Iss. 8. 085117.

16. Golesorkhtabar R., Pavone P., Spitaler J., Puschnig P., Draxl C. ElaStic: a Tool for Calculating Second-Order Elastic

Constants from First Principles. *Computer Physics Communications*. 2013. Vol. 184, Iss. 8. pp. 1861–1873.

17. Otero-de-la-Roza A., Luaña V. Gibbs2: A New Version of the Quasi-Harmonic Model Code. I. Robust Treatment of the Static Data. *Computer Physics Communications*. 2011. Vol. 182, Iss. 8. pp. 1708–1720.

18. Otero-de-la-Roza A., Abbasi-Pérez D., Luaña V. Gibbs2: A New Version of the Quasiharmonic Model Code. II. Models for Solid-State Thermodynamics, Features and Implementation. *Computer Physics Communications*. 2011. Vol. 182, Iss. 10. pp. 2232–2248.

19. Birch F. Finite Strain Isotherm and Velocities for Single-Crystal and Polycrystalline NaCl at High Pressures and 300 °K. *Journal of Geophysical Research*. 1978. Vol. 83, Iss. B3. pp. 1257–1268.

20. Erba A., Mahmoud A., Belmonte D., Dovesi R. High Pressure Elastic Properties of Minerals from *ab initio* Simulations: the Case of Pyrope, Grossular and Andradite Silicate Garnets. *The Journal of Chemical Physics*. 2014. Vol. 140, Iss. 12. 124703.

21. Nielsen O. H., Martin R. M. Stresses in Semiconductors: *ab initio* Calculations on Si, Ge, and GaAs. *Physical Review B*. 1985. Vol. 32, Iss. 6. pp. 3792–3805.

22. Hill R. The Elastic Behaviour of a Crystalline Aggregate. *Proceedings of the Physical Society. Section A*. 1952. Vol. 65, Iss. 5. pp. 349–354.

23. Voigt W. Lehrbuch der Kristallphysik (mit Ausschluss der Kristalloptik). Vieweg+Teubner Verlag, Leipzig, 1928. 979 p.

24. Reuss A. Calculation of the Flow Limits of Mixed Crystals on the Basis of the Plasticity of Monocrystals. *Zeitschrift für Angewandte Mathematik und Mechanik*. 1929. Iss. 9. pp. 49–58.

25. Xing W., Wei Z., Yu R., Meng F. Prediction of Stable High-Pressure Structures of Tantalum Nitride TaN_2. *Journal of Materials Science & Technology*. 2019. Vol. 35, Iss. 10. pp. 2297–2304.

26. Zener C. M. Elasticity and Anelasticity of Metals. Chicago: University of Chicago Press, 1948. 170 p.

27. Wu Z., Bei H., Pharr G. M., George E. P. Temperature Dependence of the Mechanical Properties of Equiatomic Solid Solution Alloys with Face-Centered Cubic Crystal Structures. *Acta Materialia*. 2014. Vol. 81, Iss. 7. pp. 428–441.

28. Osintsev K. A., Panova V. S., Kuznetsova V. A., Konovalov S. V., Panchenko I. A. First-Principles Study of the Stability of $CoCrFe_{40-x}Mn_xNi$ (x = 5, 10, 15, 20) High-Entropy Alloys. *Basic Problems of Material Science*. 2023. Vol. 20, Iss. 4. pp. 508–514.

29. Laplanche G., Gadaud P., Horst O., Otto F., Eggeler G., George E. P. Temperature Dependencies of the Elastic Moduli and Thermal Expansion Coefficient of an Equiatomic, Single-Phase CoCrFeMnNi High-Entropy Alloy. *Journal of Alloys and Compounds*. 2015. Vol. 623. pp. 348–353.

30. Klochikhin A. A., Davydov V. Yu., Seel' E. R. Compositional Fluctuations in Isotopic Solid Solutions. *Physics of the Solid State*. 2007. Vol. 49, Iss. 1. pp. 46–54.

31. Wu Z.-J., Zhao E.-J., Xiang H.-P., Hao X.-F., Liu X.-J., Meng J. Crystal Structures and Elastic Properties of Superhard IrN2 and IrN3 from First Principles. *Physical Review B*. 2007. Vol. 76, Iss. 5. 059904.

32. Korabel'nikov D. V., Zhuravlev Y. N. Ab Initio Investigations of the Elastic Properties of Chlorates and Perchlorates. *Physics of the Solid State*. 2016. Vol. 58, Iss. 6. pp. 1166–1171.

33. Liu H., Xin C., Liu L., Zhuang C. Effects of Different Contents of Each Component on the Structural Stability and Mechanical Properties of Co – Cr – Fe – Ni High-Entropy Alloys. *Applied Sciences*. 2021. Vol. 11, Iss. 6. 2832.

34. Boucetta S. Theoretical Study of Elastic, Mechanical and Thermodynamic Properties of MgRh Intermetallic Compound. *Journal of Magnesium and Alloys*. 2014. Vol. 2, Iss. 1. pp. 59–63.

35. Tian F., Varga L. K., Shen J., Vitos L. Calculating Elastic Constants in High-Entropy Alloys Using the Coherent Potential Approximation: Current Issues and Errors. *Computational Materials Science*. 2016. Vol. 111. pp. 350–358. NFM